Confocal Microscopy with Optimized Excitation and Emission Wavelength for Ultradeep and Multi-channel Bioimaging: Supplementary Information

Tianxiang Wu[1], Weihang Geng[1] , Yuhuang Zhang[1], Qiming Xia[2], Mingxi Zhang[3], Jin Li[4] , Menglu Chen[5], Wang Xi[6], Shiyi Peng[1], Zhe Feng[1], Jun Qian[1,*]

[1] State Key Laboratory of Extreme Photonics and Instrumentation, Centre for Optical and Electromagnetic Research, College of Optical Science and Engineering, International Research Center for Advanced Photonics, Zhejiang University, 310058, Hangzhou, China

[2] Department of General Surgery, Sir Run Run Shaw Hospital, Zhejiang University School of Medicine, Hangzhou 310016, China

[3] State Key Laboratory of Advanced Technology for Materials Synthesis and Processing, Wuhan University of Technology, Wuhan 430070, China

[4] State Key Laboratory Breeding Base of Green-Chemical Synthesis Technology, Institute of Green Petroleum Processing and Light Hydrocarbon, College of Chemical Engineering, Zhejiang University of Technology, Hangzhou 310014, China

[5] School of Optics and Photonics, Beijing Institute of Technology, Beijing, 100081, China

Westlake Institute for Optoelectronics, Fuyang, Hangzhou, 311421, China

[6] Interdisciplinary Institute of Neuroscience and Technology (ZIINT), the Second Affiliated Hospital, School of Medicine, Zhejiang University, Hangzhou, 310020 China

* qianjun@zju.edu.cn

Supplementary Methods

Fluorescence collection assessment of confocal microscopy based on Monte Carlo simulation

To investigate the influence of fluorescence bands on confocal imaging signal collection, the Monte Carlo method was employed to assess fluorescence collection efficiency. This simulation approach builds upon our previous work [1], with modifications to the imaging system as depicted in **Figure S1**.

To mitigate the impact of excitation light in the simulation, the excitation light was configured to stimulate the fluorescent material within the tissue using an ideal spatial cone. The ensuing fluorescence then propagated through the objective lens (25x, NA=1.05), tube lens (f=200 mm), scan lens (f=50 mm), and a final lens (f=10 mm), culminating at the pinhole (Φ9 μm).The tissues used in the simulation have scattering coefficient data from mouse brain tissue and absorption coefficient data from water.Fluorescent photons were recorded exclusively when they traversed the pinhole and reached the detector. For instance, at a wavelength of 1300 nm, the energy distribution of the excitation light within the tissue is illustrated in **Figure S2**b. The spatial distribution of fluorescent photons that successfully passed through the confocal pinhole to the detector is depicted in **Figure S2**c. The fluorescence light intensity distribution along the optical axis is presented in **Figure S2**d. A depth of 1 μm was selected as the chromatographic target, with signals beyond this range being attributed to background noise due to factors such as tissue scattering. By varying the fluorescence wavelength and calculating the ratio of fluorescence intensity within the central depth range, a confocal effective collection spectrum was derived, as shown in **Figure S2**e. This spectrum elucidates the variations in confocal image quality across different fluorescence wavelength.

Supplementary Figures

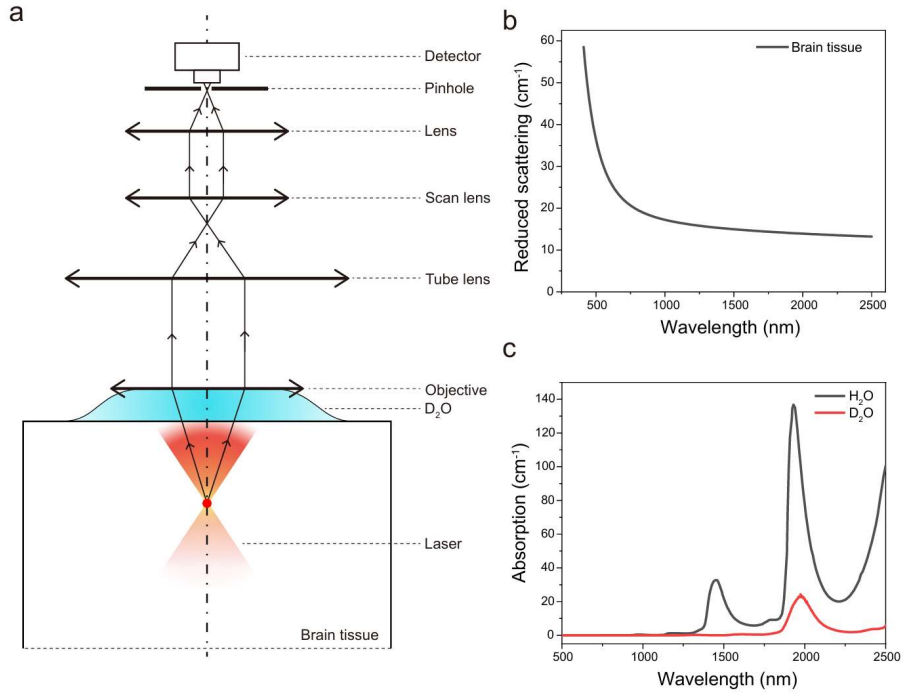

Figure S1 System and parameterization for Monte Carlo simulations. (a) Schematic of the optical path

for the simulation. (b) Reduced scattering spectra of mouse brain tissue [2]. (c) Absorption spectra of water and heavy water.

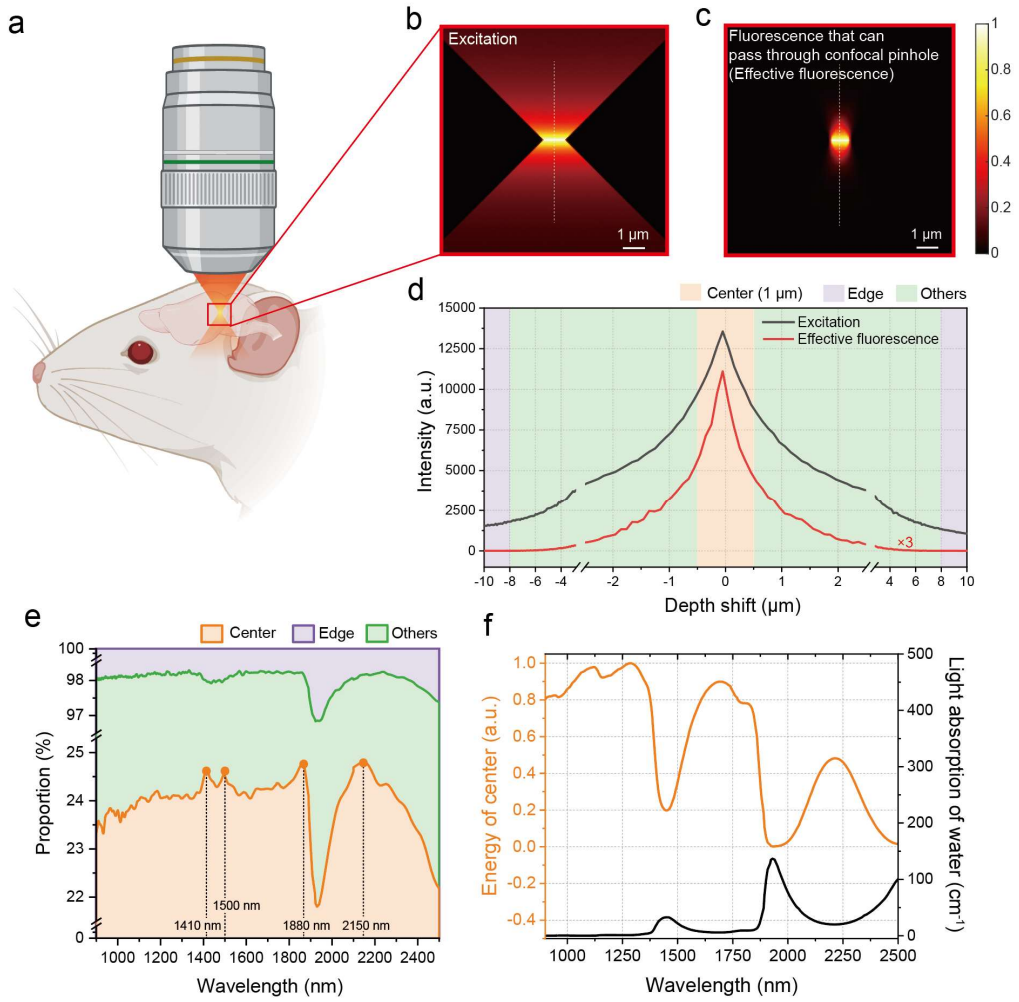

Figure S2. Conclusion of Monte Carlo-based simulation of NIR-II fluorescence confocal microscopy. (a) Schematic representation of the actual imaging scene corresponding to the simulation. (b) Spatial intensity distribution of the excitation light as depicted in the simulation. (c) Spatial intensity distribution of the fluorescence signal that can successfully traverse the pinhole to reach the detector. (d) Spatial intensity distribution of excitation and fluorescence light along the optical axis (along the dash line in (b) and (c)), and the light intensity in the range within the central 1 μm depth was considered as effective signal, as indicated by the yellow background. The energy distribution with depth shift beyond 8 μm from the focal point was labeled "Edge" and is shown in purple. Other areas were labeled "Others" and are depicted in light green. (e) Spectra showing the effective energy collection proportion of NIR-II fluorescence confocal microscopy. The effective energy exhibits extreme values at 1410, 1500, 1880, and 2150 nm, indicating better tomographic capabilities for confocal microscopic imaging with fluorescence of these wavelength. (f) Comparison of the effective collection efficiency spectrum of confocal microscopy and the water absorption spectrum, demonstrating a correlation at local extremes

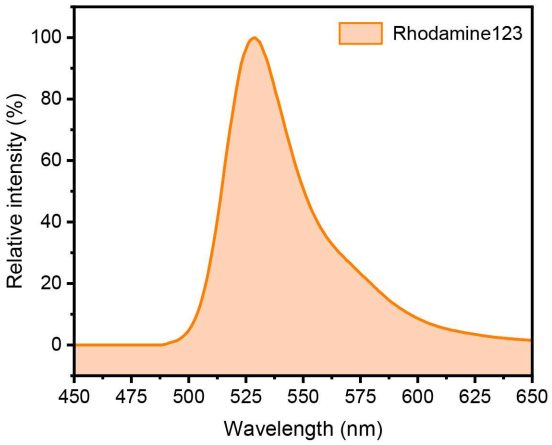

Figure S3 Fluorescence emission spectrum of Rhodamine123.

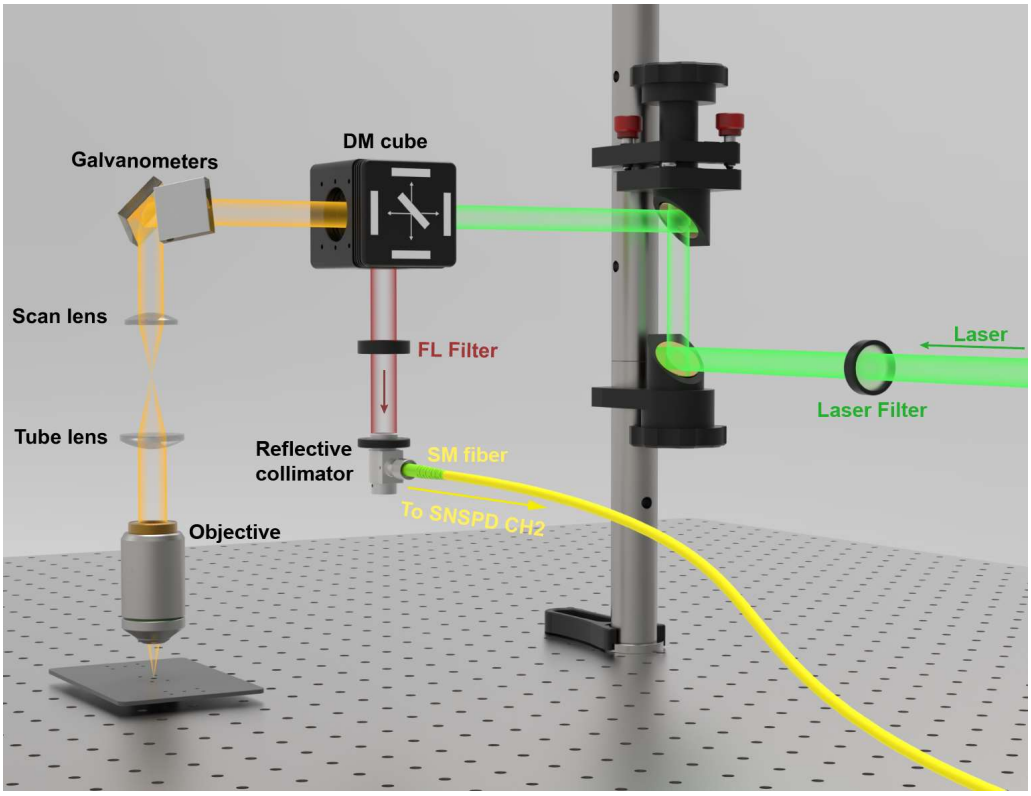

Figure S4 Schematic representation of the NIR-II fluorescence confocal microscope.

The laser light was directed through the DM Cube and into the microscope (FVMPE-RS, Olympus, Japan), where it was sequentially focused onto the sample via galvanometers, a scan lens, a tube lens, and an objective lens. The emitted fluorescence retraces its path through the objective lens, tube lens, scan lens, and galvanometers back to the DM Cube. There, it is deflected downward, passes through a filter, and is then collimated by a reflective collimator into an optical fiber for transmission to the detector (SNSPD).

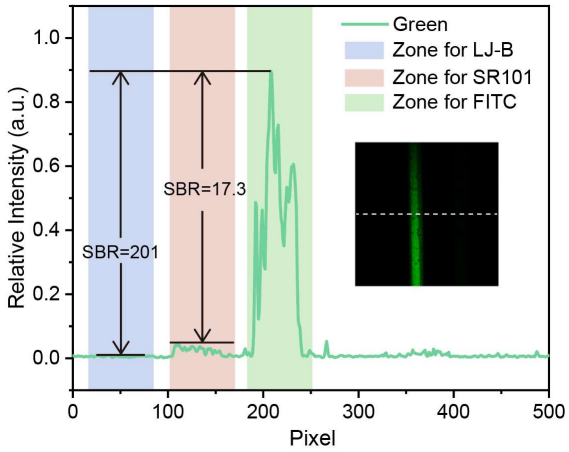

Figure S5 Crosstalk Analysis of green Channels. The inset in the figure shows the green channel imaging, with image intensity analyzed along the white dashed line. When trailing green fluorescence signals of LJ-B and SR-101 are regarded as background noise for the green fluorescence signal of FITC, the signal-to-noise ratios for FITC/LJ-B and FITC/SR-101 are estimated to be approximately 201 and 17.3, showing very little inter-channel crosstalk.

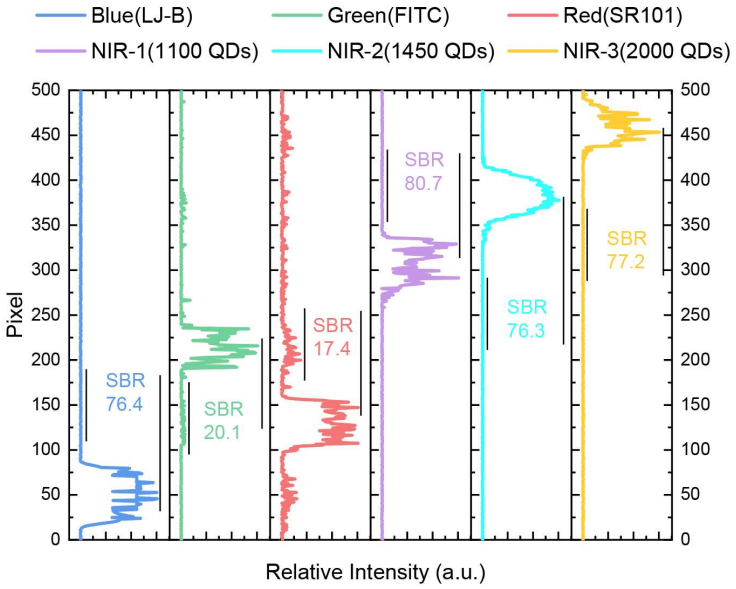

Figure S6 Crosstalk Analysis Between Channels. Data were extracted from the intensity profiles of each channel along the horizontal axis in the in vitro multi-channel microscopic imaging (Figure 3b in revised manuscript). To calculate the SBR for a single channel, the maximum signal intensity of that channel is used as signal. The channel with the highest background noise among the other five is selected, and its maximum noise value is taken as the background noise intensity. The SBR is then determined by dividing the signal intensity by the background noise intensity.

References

1. Wu, T.; Wang, Y.; Lin, H.; Qian, J., A Pervasive Approach for Determining the Optimal Tissue Windows for Near-Infrared Fluorescence Imaging. *Laser & Photonics Reviews* **2024,** *10* (15), 2400628.

2. Al-Juboori, S. I.; Dondzillo, A.; Stubblefield, E. A.; Felsen, G.; Lei, T. C.; Klug, A., Light Scattering Properties Vary across Different Regions of the Adult Mouse Brain. *Plos One* **2013,** *8* (7).